Traffic

Published by John Wiley & Sons Ltd
doi:10.1111/tra.12243

Intrinsically Disordered Linker and Plasma Membrane-Binding Motif Sort Ist2 and Ssy1 to Junctions

Annemarie Kralt[1], Marco Carretta[1,2], Muriel Mari[3], Fulvio Reggiori[3], Anton Steen[1], Bert Poolman[4] and Liesbeth M. Veenhoff[1,*]

[1]European Institute for the Biology of Ageing (ERIBA), University of Groningen, University Medical Center Groningen, Netherlands Proteomics Centre, Antonius Deusinglaan 1, 9713 AV, Groningen, The Netherlands
[2]Current address: Department of Hematology, University of Groningen, Hanzeplein 1, 9713 GZ Groningen, The Netherlands
[3]Department of Cell Biology, Center for Molecular Medicine, University Medical Center Utrecht, Heidelberglaan 100, 3584 CX, Utrecht, The Netherlands
[4]Department of Biochemistry, University of Groningen, Nijenborgh 4, 9747 AG, Groningen, The Netherlands
*Corresponding author: Liesbeth M. Veenhoff, l.m.veenhoff@rug.nl

Abstract

Membrane junctions or contact sites are close associations of lipid bilayers of heterologous organelles. Ist2 is an endoplasmic reticulum (ER)-resident transmembrane protein that mediates associations between the plasma membrane (PM) and the cortical ER (cER) in baker's yeast. We asked the question what structure in Ist2 bridges the up to 30 nm distance between the PM and the cER and we noted that the region spacing the transmembrane domain from the cortical sorting signal interacting with the PM is predicted to be intrinsically disordered (ID). In Ssy1, a protein that was not previously described to reside at membrane junctions, we recognized a domain organization similar to that in Ist2. We found that the localization of both Ist2 and Ssy1 at the cell periphery depends on the presence of a PM-binding domain, an ID linker region of sufficient length and a transmembrane domain that most probably resides in the ER. We show for the first time that an ID amino acid domain bridges adjacent heterologous membranes. The length and flexibility of ID domains make them uniquely eligible for spanning large distances, and we suggest that this domain structure occurs more frequently in proteins that mediate the formation of membrane contact sites.

Keywords amino acid signaling, endoplasmic reticulum, intrinsic disorder, membrane junction, membrane protein trafficking, plasma membrane

Received 4 April 2014, revised and accepted for publication 18 November 2014, uncorrected manuscript published online 20 November 2014, published online 28 December 2014

With the evolution of membrane-bound organelles, multiple possibilities for orchestrating molecular processes in defined microenvironments arose. Several means of communication between these organelles evolved to coordinate these processes. One of them is through the formation of direct contact sites between their membranes (1–4). Contact sites were already described in the 1950s and defined as heterologous membranes positioned within a distance of 30 nm of each other, which is based on the notion that such a distance can potentially be spanned by a protein complex (3,5). Molecular players involved in the formation and the relevance of contact sites have been unraveled more recently (reviewed in 6). In the yeast *Saccharomyces cerevisiae,* extensive contact sites are formed between the plasma membrane (PM) and the cortical endoplasmic reticulum (cER) (4,7). One of the proteins involved in establishing these connections is Ist2. Upon deletion of Ist2, the PM and the cER separate, while upon its overexpression, the number of cER–PM junctions increases (5,8,9). Additionally, Ist2 from *S. cerevisiae* expressed in

mammalian cells also induces the formation of contact sites between the PM and the ER (10).

Initially, the eight transmembrane (TM) segments of Ist2 were thought to be inserted in the PM based on subcellular fractionation and protease protection data (11). The current view, however, is that an amphipathic α-helix in the C-terminal cortical sorting signal (CSS) of Ist2 functions as a PM-binding (PMB) domain, whereas its TM domain is in the cER (5,8,9,12). Data supporting this topology of Ist2 are that, (i) the targeting of this protein to the cell periphery does not rely on the conventional secretory pathways (13,14), (ii) the CSS amphipathic α-helix is able to bind PM-like liposomes and (iii) mutation of the CSS reduces the localization of Ist2 at peripheral membranes and increases perinuclear localization of the protein (12). We noted that approximately 300 amino acid residues of Ist2, between the TM domain and the CSS, are predicted to be intrinsically disordered (ID). ID regions lack persistent secondary or tertiary structure, and, because they are flexible and long, we reasoned that they potentially function as a linker region connecting the PM and the ER.

Ssy1 shares its peripheral localization with Ist2, and we detected that the N-terminal region contains a putative PMB domain, a stretch of positively charged amino acids and a putative ID linker region. Ssy1 forms the SPS (Ssy1-Ptr3-Ssy5) sensor complex together with Ptr3 and Ssy5 (15,16) that senses amino acids and induces the transcription of several amino acid permeases (AAPs) (17,18). Ssy1 is a unique member of the protein family (19) as it does not transport amino acids (15,17). Moreover, its very long N-terminal domain, encoding the putative PMB domain and ID linker region, is absent in other AAPs and has a role in sensor functioning (20).

Here, we investigated the localization of these two proteins, Ssy1 and Ist2, to the cell periphery. Our localization and subcellular fractionation data indicate that Ssy1 is an ER-resident protein, localized to the cER and interacting with the PM, like Ist2. The ID region of both Ist2 and Ssy1 can be replaced by an alternative disordered region of sufficient length without altering their localization, consistent with its function to bridge the PM and the cER. Altogether, our data reveal that localization of Ist2 and Ssy1 to PM–cER junctions depends on a module composed of (i) a PM-binding domain; (ii) an ID linker region that could function to bridge the distance between the two adjacent membranes and (iii) ER-embedded TM segments.

Results

The role of a putative ID region in Ist2 localization to the PM–ER junctions

We first tested the hypothesis that the predicted ID region in Ist2, between the TM domain and the CSS (Figure 1A), may function as a linker to span the distance between the PM and the cER membrane. For a simple linker function, the biophysical parameters such as flexibility and Stokes radius are expected to be relevant but not the exact amino acid sequence. We constructed a gene in which the region encoding for the ID region (between amino acids 596 and 917) was replaced by a synthetic fragment of DNA that encoded a randomized version of the original amino acid sequence. The resulting ID linker thus shared with the native linker its disorder-promoting amino acid composition, but was entirely different in its amino acid sequence. N-terminal GFP fusions of Ist2 and Ist2 with a randomized ID region (Ist2RL) were expressed in the *ist2*Δ background and localization of the proteins was visualized with fluorescence microscopy. Indeed, Ist2RL revealed the same localization at the cell periphery as that by Ist2 (Figure 1B), and we concluded that a sequence-randomized disordered linker supports localization to PM–ER junctions, consistent with a linker function.

The ID region between the TM domain and the amphipathic helix (residues 589–928) is 340 amino acids long. To investigate the importance of the linker length, we generated Ist2 internal truncations, leaving linkers of 240, 140 and 58 residues in length (Ist2L240, Ist2L140 and Ist2L058, respectively). All truncations were expressed to similar levels (Figure S1B) and were only found at the cell periphery, but to different degrees. While Ist2L240 was distributed to the cell periphery as was Ist2, Ist2L058 was localized to small, discrete puncta (Figure 1B). Furthermore, we observed a slight difference between the localization of Ist2 and Ist2L140: the sizes of the patches that were formed at the periphery were smaller in Ist2L140 and regions of low fluorescence were larger (Figure 1B).

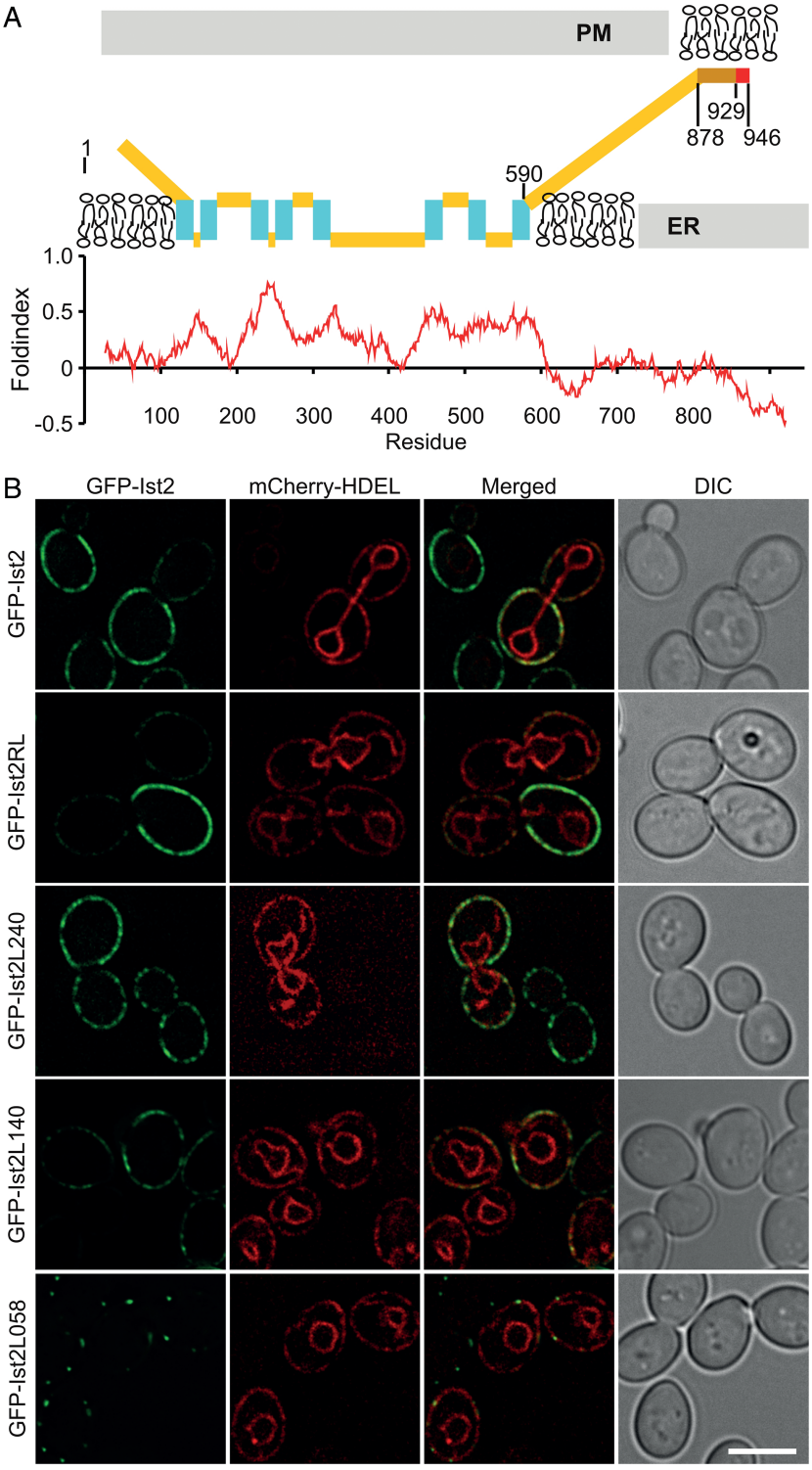

Figure 1: Localization of Ist2 and ID linker mutants. A) Schematic representation of Ist2, containing 8 TM segments (blue) and a long C-terminal domain with poor folding probability as is shown in the Foldindex© graph. The C-terminal cortical sorting signal is shown in orange (basic cluster) and red (amphipathic helix). B) Fluorescent images of N-terminal GFP fusions of Ist2 driven by the Ist2 promoter (green) and the *GAL1*-induced ER marker mCherry-HDEL (red). Wild-type Ist2 (GFP-Ist2), Ist2 with a randomized linker region (GFP-Ist2RL) and Ist2 with truncated linkers (GFP-Ist2L240, GFP-Ist2L140, GFP-Ist2L058, respectively) are shown. Scale bar represents 5 μm.

The differences in localization are subtle and so, as a measure for the distribution of the protein at the periphery, we determined the normalized standard deviation of the pixel intensity along the periphery of 90 cells. In cells expressing Ist2L140, this value was significantly higher ($p < 10^{-5}$) than that in cells expressing Ist2 or Ist2RL (Figure S2), indicating that Ist2 with reduced linker length was distributed less homogenously over the periphery.

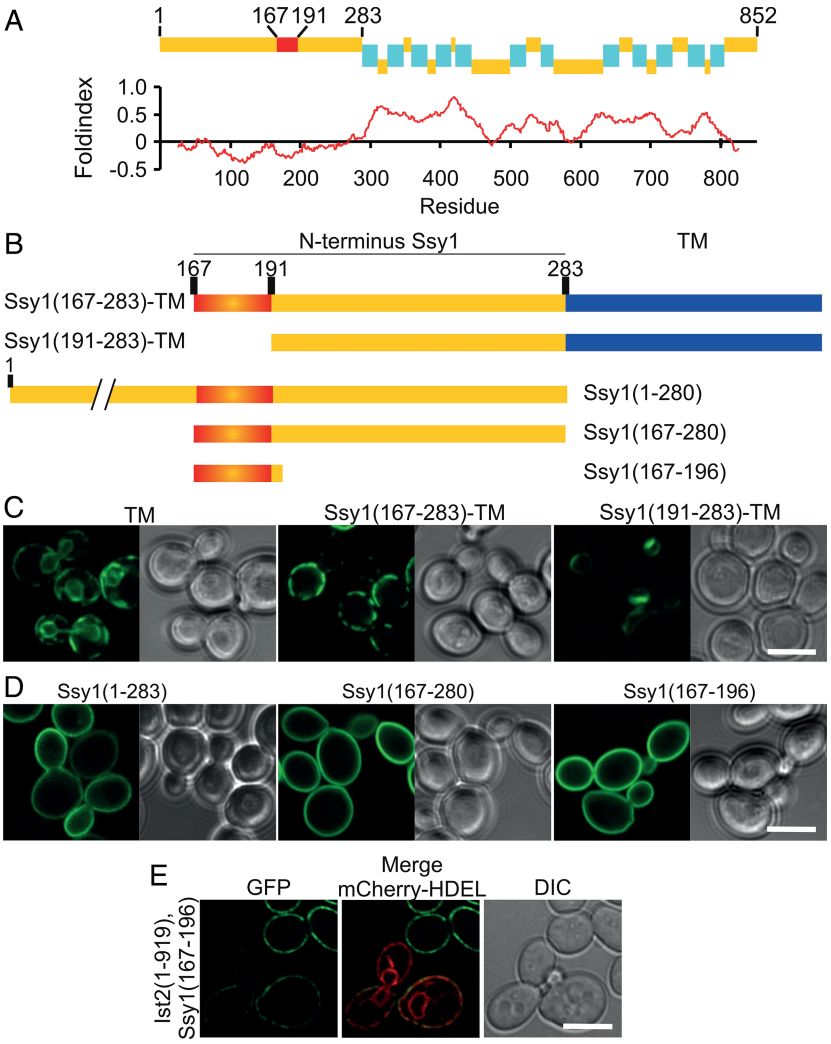

Figure 2: Sorting signals in N-terminus of Ssy1 sort to cell periphery. A) Schematic representation of Ssy1 with the TM segments represented as blue bars and in red the PMB domain consisting of positive residues. The Foldindex© graph below shows that the N-terminus of Ssy1 is predicted to have poor folding capabilities. B) Schematic representation of truncations made of the N-terminus of Ssy1, with the PMB domain shown in red. All proteins are N-terminally fused to GFP and *GAL1*-induced for 4 h. C) The TM domain alone localizes to the NE–ER network (C, left), while Ssy1(167–283)-TM localizes to the cell periphery (C, middle). Peripheral localization is lost upon removal of the PMB domain (C, right). D) The N-terminus or truncations thereof target GFP to the cell periphery, and only residues 167–196 are sufficient to establish this attachment. E) Peripheral localization of Ist2 is supported after replacement of the amphipathic helix of Ist2 by the PMB domain of Ssy1 (167–196). Scale bar represents 5 μm.

Altogether, we concluded that the length of the linker region between the TM domain and the CSS is of interest for targeting of Ist2 to the cell periphery, rather than the amino acid sequence. Together with previous data on the embedding of the TM domain in the ER and the amphipathic helix binding the PM (8,9,12,14), our results support the model that the predicted ID region between these two domains functions as a linker spanning the distance between the cER and the PM.

The N-terminus sorts Ssy1 to the cell periphery

In Ssy1, which localizes to the cell periphery, we recognized a similar combination of domains as that in Ist2, i.e. a putative PMB domain, which is composed of a stretch of positive amino acids followed by an ID region and a TM domain (Figure 2A). We thus tested whether the N-terminus of Ssy1 can target a TM segment to the periphery by fusing it with a TM segment derived from the yeast protein Heh2 (Figure 2B). The TM alone localized to the NE–ER network as anticipated (Figure 2C, TM), but, when fused with the region encoding the sequence of the putative PMD domain and the ID linker region of Ssy1 (residues 167–283), it was targeted to patches at the cell periphery [Figure 2C, Ssy1(167–283)-TM], where the protein colocalizes with the cER (Figure S3). Upon removal of the putative PMB domain [Ssy1(191–283)-TM], the peripheral localization of the reporter protein was completely abolished (Figure 2C). We note that the high perinuclear fluorescence in cells expressing Ssy1(191–283)-TM is a result of the induction of membrane stacks at the NE (Figure S4). This is a phenotype that we do not understand, but have observed previously when overexpressing various

NE/ER-resident proteins with various ID linkers and transmembrane domains.

Consistent with the notion that the positive residues in the putative PMB domain of Ssy1 interact with one or more components of the PM, the entire N-terminus (1–280), the putative 'PMB-ID linker' region (167–283) or solely the 30-amino acid long sequence (167–196) efficiently sorted GFP to the PM (Figure 2D). Finally, we asked whether the PMB domain of Ssy1 could support localization of the Ist2 variant lacking its CSS [Ist2(1–919)] to the cell periphery. Indeed Ist2(1–919) mutant fused with the PMB domain of Ssy1[Ist2(1–919)], Ssy1(167–196) localized to the cER in a similar fashion as the protein with the native CSS (Figures 2E and S2). From these studies, we concluded that the N-terminus of Ssy1 sorts a TM segment to the cell periphery and encodes a PMB sequence.

We next asked whether the recruitment of Ssy1 to the periphery is because of either a PM tethering of an ER-resident TM domain, like for Ist2, or the TM domain inserting into the PM. Several reports have argued that the TM of full-length Ssy1 is inserted into the PM, but our results prompted us to re-evaluate the topology and localization of this protein. We performed membrane fractionation studies to determine the localization of Ssy1. We used a functional HA-tagged version of Ssy1 expressed from its native promoter, described in (16). The protein fractionated in two peaks (around fractions 3–5 and around fractions 7–8), which were close to the ER marker protein Dpm1 (fractions 5–8) but not to the PM marker protein Pma1 (fractions 11–14) (Figures 3A and S5, HKY20). A similar trend was observed in a mutant strain lacking the chaperone protein Shr3 (Figure 3B and S5, HKY29), which is involved in correct folding and packaging of transport vesicles (21,22). That is, the fractionation pattern of Ssy1 (fractions 2–7) did not overlap with that of Pma1 (fractions 9–12). Although differences in sedimentation profiles were observed depending on the buffer composition, no co-fractionation of Ssy1 with Pma1 was found in any of the tested conditions (Figure S5). The reason for the different fractionation behaviors reported previously (16) is not clear to us.

Genomically, GFP-tagged Ssy1 could not be detected by fluorescence microscopy because of its very low expression level, and so we visualized the distribution of this fusion protein under the control of the galactose promoter *GAL1*. GFP-Ssy1 localized to the entire nuclear envelope–ER (NE–ER) network and also to the puncta at the cell periphery (Figure 3C), as also illustrated in the 3D projection (Figure 3D). Full-length GFP-Ssy1 is thus not significantly enriched at ER–PM contact sites when overexpressed. This may be an overexpression artifact or the distribution of the endogenous protein: it may be that, unlike Ist2, only a small fraction of endogenous Ssy1 is located at ER–PM contact sites.

Altogether, a definitive answer to the question if native Ssy1 is in the ER membrane or the PM is not readily obtained from these experiments, but our subcellular fractionation and microscopy data were most compatible with Ssy1 being an ER integral membrane protein and argue against it being embedded in the PM.

Expression of Ssy1(167–283)-TM induces association between ER and PM

We addressed the effect of expression of Ssy1(167–283)-TM in a strain that lacked six proteins involved in PM–ER tethering (8). In this strain, named Δtether, the morphology of the cER is altered, and the ER is no longer predominantly found at the cell periphery but now accumulates in the cytoplasm. We asked whether expression of Ssy1(167–283)-TM could restore PM–ER contact sites in the Δtether strain. Indeed, with fluorescence microscopy, we observed that in the Δtether strain, the ER appeared collapsed (Figure 4A, top), and as previously reported (8), and expression of Ssy1(167–283)-TM resulted in substantial amounts of ER underlying the PM (Figure 4A, bottom). Electron microscopy was then used to visualize the ER and PM associations at the ultrastructural level. In the Δtether strain, most of the ER accumulated around the nucleus consistent with (8), but when in the Δtether strain Ssy1(167–283)-TM was expressed, close associations between PM and ER were observed (Figure 4B), showing that Ssy1(167–283)-TM restored PM–ER associations in the Δtether strain.

Consistently, we observed that in a wild-type strain, associations of the PM with the ER were induced upon overexpression of Ssy1(167–283)-TM. While in the wild-type strain, the cER appeared to be normal in terms of proximity

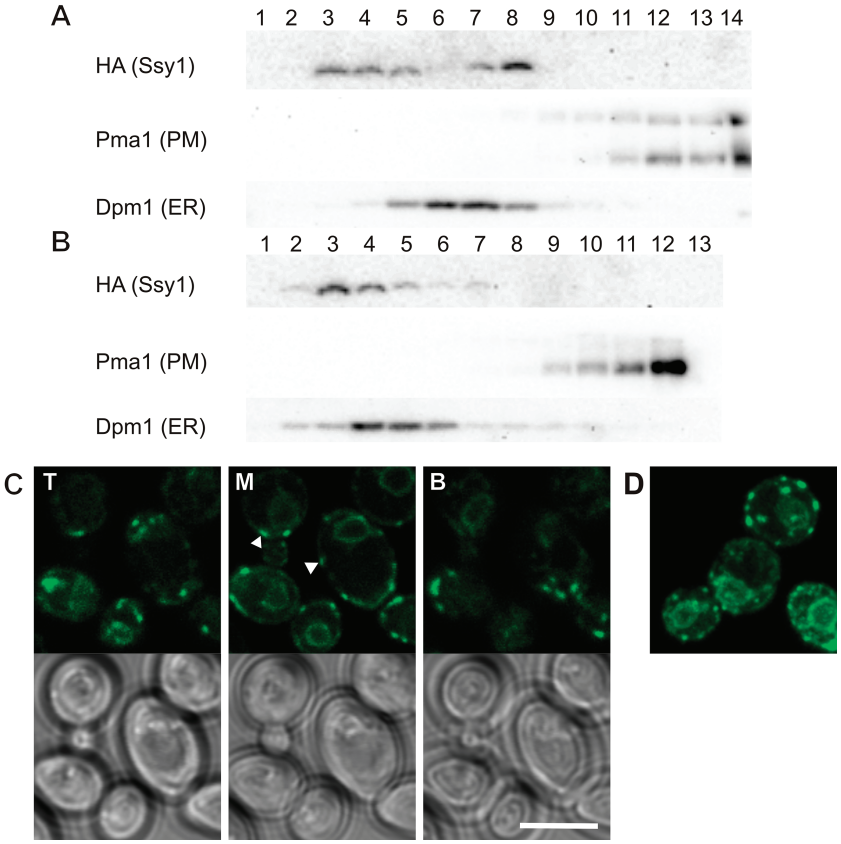

Figure 3: Subcellular fractionation of native levels of Ssy1 and localization of overexpressed Ssy1. Membrane fractionation over sucrose gradients of cell lysates of HKY20 (*ssy1Δ13*) (A) and of cell lysates of HKY29 (*ssy1Δ13 shr3Δ6*) (B) expressing a functional HA-tagged allele of *SSY1* (pHK010). Proteins in the fractions are separated by SDS-PAGE and analyzed by immunoblotting. Ssy1 does not cofractionate with the PM marker Pma1, but overlaps more with the ER marker Dpm1. C) The top (T), middle (M) and bottom (B) of cells expressing *GAL1*-induced GFP-Ssy1. GFP-Ssy1 mainly localizes to the NE–ER network, but also accumulates in spots at the periphery as is indicated with arrow heads. D) This localization in peripheral spots is visualized in a 3D projection of the localization of GFP-Ssy1. Scale bar represents 5 μm.

to the PM and was non-continuous (Figure 5A,C), cells expressing Ssy1(167–283)-TM displayed continuous cER and very closely opposed to the PM (Figure 5B,D). Both in the wild-type and the Δtether background, the distance between the cortical ER and the PM at these sites was too small to be measured. In the wild-type background, in few occasions, the cER membrane appeared to be relatively thick, indicating that there could be more than one ER leaflet. A second effect of expression of Ssy1(167–283)-TM on the morphology, both in the wild-type and the Δtether background, was that areas with expanded and irregular cell wall were observed (Figure 5B). These areas were always present in the cell regions where there was cER aligned to the PM, possibly indicating that excessive cER tethering with the PM disrupts processes like endocytosis and exocytosis, and/or cell wall biogenesis. We concluded from the electron microscopy and fluorescence microscopy data that overexpression of Ssy1(167–283)-TM induces a prominent intimate association between the ER and the PM in wild-type strains while restoring peripheral localization of the otherwise collapsed ER in the Δtether strain.

Tuning peripheral targeting by mutagenesis of the ID region and the PMB domain

In Ist2, the ID region acts as a linker to span the PM and the ER membrane. We thus explored whether the predicted ID region spacing the TM and PMB domain of Ssy1 could also act as a linker. Therefore, we replaced this region by an unrelated ID region of the same length in Ssy1(167–283)-TM. Indeed, the protein with the replaced linker region ['exchanged linker', Ssy(167–191)RL87-TM] localized to the cell periphery in the same way as the protein with Ssy1(167–283)-TM (Figure 6A). Interestingly, when the linker region (residues 197–271) was removed from this reporter protein, the localization of the protein became dependent on galactose induction time. While Ssy1(167–283)-TM or Ssy(167–191)RL87-TM does not change its localization with prolonged induction time, the protein without the linker first localized to the NE–ER network, but peripheral patches start to appear after 4 h of induction, which then increased in size at the 20 h induction time (Figure 6B). Those patches were increased in size compared with the size of the patches that are formed in the presence of the full-length linker, and cover only parts

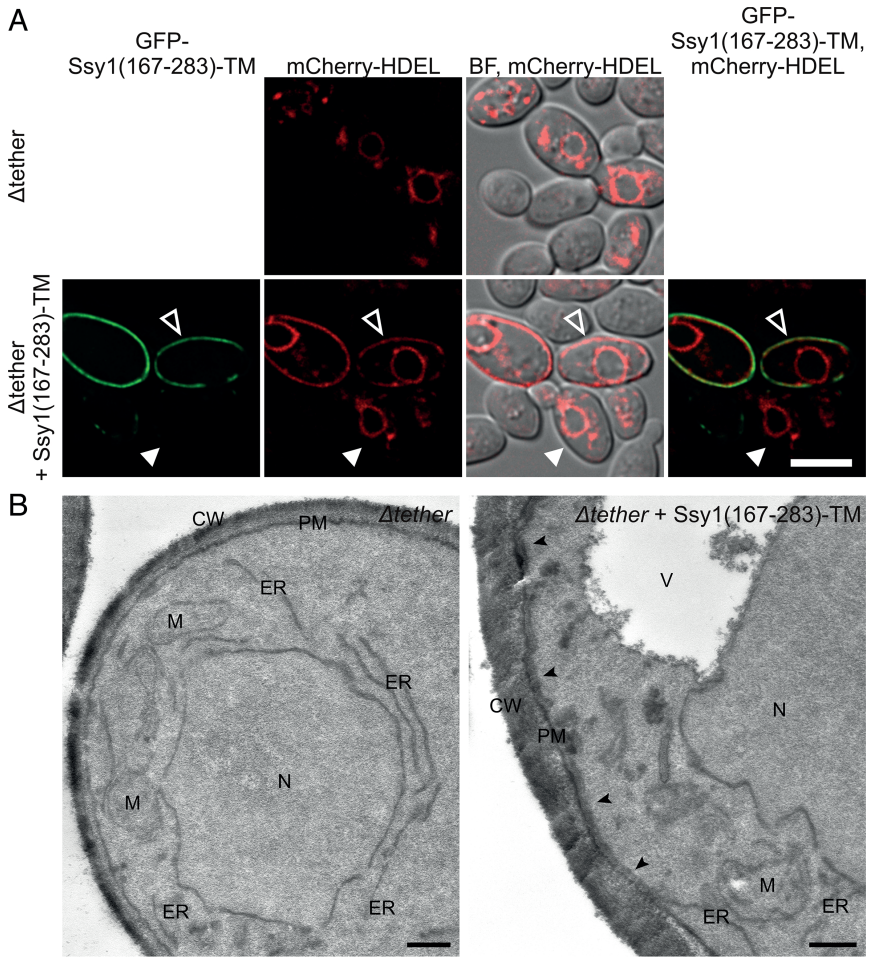

Figure 4: PM–ER contact sites are restored in the Δtether strain by Ssy1(167–283)-TM. A) The ER in the Δtether strain, which lacks 6 proteins that mediate the formation of PM–ER contact sites, is visualized with an ER marker fused to mCherry. In the Δtether strain, the ER accumulates in the cytoplasm. Upon expression of Ssy1(167–283)-TM cortical ER appeared colocalizing with the reporter protein (open arrow head), while in cells with no apparent expression of Ssy1(167–283)-TM (closed arrowhead), the ER still accumulates in the cytoplasm. Scale bar represents 5 μm. B) Ultrastructural analysis of the Δtether strain without (left panel) and with (right panel) expressing Ssy1(167–283)-TM. Cortical ER appears when Ssy1(167–283)-TM is expressed as is indicated with the arrow heads. CW, cell wall; ER, endoplasmic reticulum; M, mitochondria; N, nucleus; V, vacuole. Scale bars represent 200 nm.

of the cell periphery. We concluded that an unrelated ID linker supports localization of Ssy1-derived TM reporters to the cell periphery. Moreover, we also established that a shortened linker is less efficient in sorting proteins to the cell periphery.

To investigate the interaction of the PMB with the PM, we performed mutant analysis, and asked if mutagenesis of the basic clusters would result in reduced affinity of the PMB domain to the PM and subsequently would affect the peripheral localization of soluble and membrane proteins. The arginines and lysines present in the PMB domain were substituted by alanines in various combinations (Figure 7A). When those changes were introduced into the soluble N-terminus of Ssy1 [Ssy1(167–280)], we observed a gradual decrease of protein amounts attached to the PM, with the most dramatic effect in the construct in which all the positive residues were mutated (e.g. 10A, Figure 7B,C). When the mutations were introduced in the membrane-embedded fusions, the effects were even stronger. When five residues of the PMB domain were changed into alanines, targeting to the periphery was affected, i.e. the chimera mostly localized to the nuclear envelope and only few spots were observed at the cell periphery (Figure 7D). When 10 alanines were introduced in the PMB domain, the peripheral localization was completely abolished (Figure 7E). So, while soluble 8A mutants still effectively sort to the PM, peripheral sorting of the 5A mutant is highly compromised. We concluded that weakening the PMB affinity for the PM affected most strongly the sorting of TM proteins.

Altogether, we showed that the C- and N-termini of Ist2 and Ssy1, respectively, encode a PMB domain and an ID linker region that together are required for the targeting of these proteins to the cell periphery. In both cases, our data support a topological organization where the TM domain embedded into the cER is connected to a sequence that

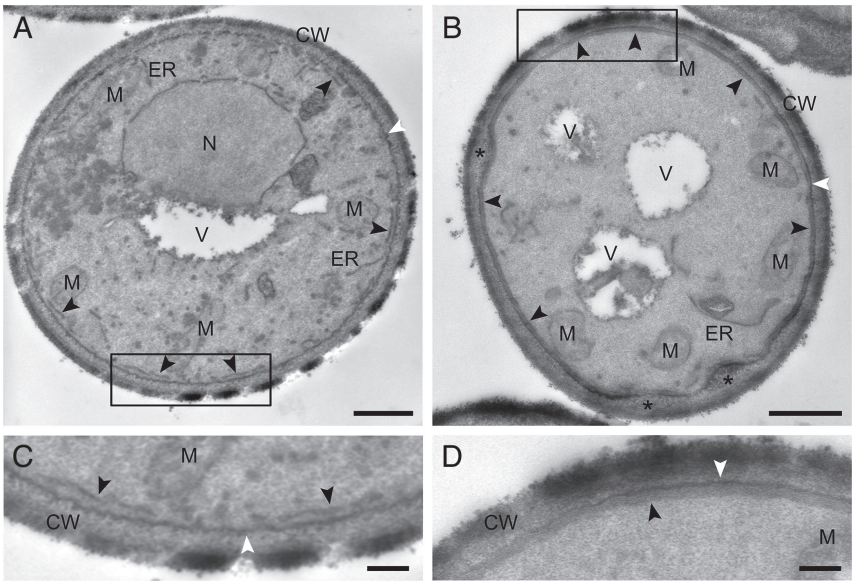

Figure 5: Ultrastructural analysis of wild-type cells expressing Ssy(167–283)-TM. The W303 strain expressing GFP-Ssy1(167–283)-TM (B and D) or not (A and C) was processed for electron microscopy as described in Materials and Methods. The PM is indicated with a white arrow head while the cER is indicated with a black arrow head. Asterisks indicate areas where the cell wall is swollen in the cells expressing GFP-Ssy1(167–283)-TM. Area highlighted by a square in panels A and B. CW, cell wall; ER, endoplasmic reticulum; M, mitochondria; N, nucleus; V, vacuole. Scale bars represent 500 nm (A) and 200 nm (B).

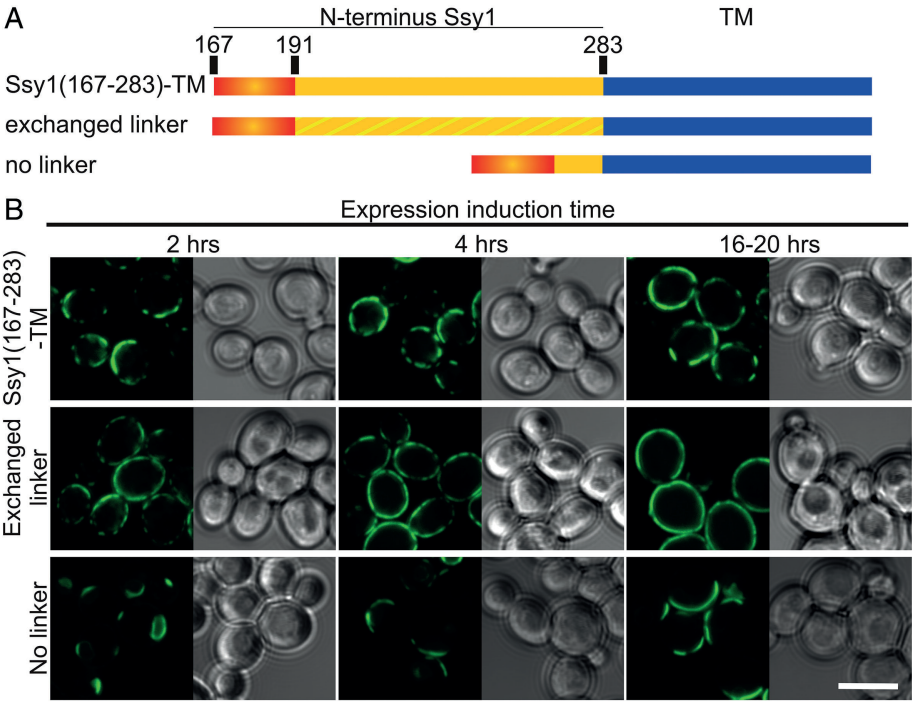

Figure 6: ID linker length but not sequence affects sorting to the periphery. A) Schematic representation of truncations made of the N-terminus of Ssy1. All proteins are N-terminally fused to GFP and *GAL1*-induced. B) An unrelated ID linker supports localization to the cortical ER (exchanged linker). Removal of the linker (no linker) results in a delayed localization at the cortical ER and the patches do not extend over large areas of the periphery. Scale bar represents 5 μm.

binds the PM by an ID linker. We named this structural module a 'membrane-tethering module'.

Discussion

We have uncovered a role for intrinsically disordered linkers in sorting the membrane proteins Ist2 and Ssy1 to the cell periphery. Ist2 and Ssy1 are unrelated in structure and function, but both localize to the cell periphery. Ist2 was first described as a PM protein, but more recent data support residency of its TM domain in the cER while its C-terminal CSS binds to PM lipids (13,14). This domain architecture of Ist2 sorts the protein to the cell periphery and tethers the cER with the PM. Ssy1 was described to be present at the PM as well, and this seemed logical regarding its function as a sensor for the presence of amino acids and its homology to PM-localized AAPs (17,18). Our subcellular fractionation results, however, argue

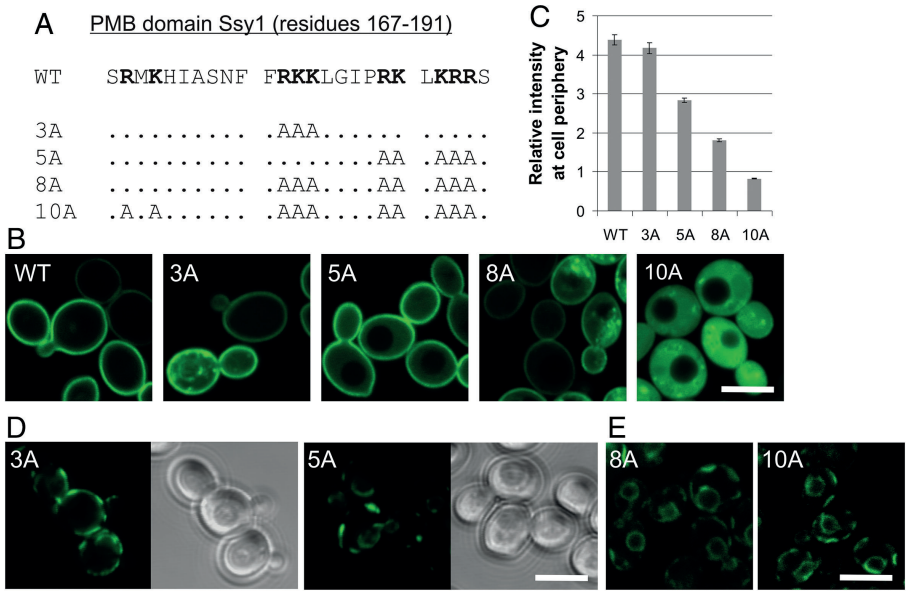

Figure 7: Mutations in the positive residues of the PMB domain of Ssy1(167–283) decrease attachment to the PM. A) Alanine substitutions that are made in the PMB domain. B) Localization of Ssy1(167–283) with and without mutations in the PMB domain. C) Quantification of the decrease in peripheral localized protein. The ratio of fluorescence intensity at the periphery over the fluorescence intensity at the cytoplasm is plotted. D and E) Progressive loss of peripheral localization of Ssy1(167–283)-TM with 3, 5, 8 and 10 alanine substitutions. Scale bars represent 5 μm.

against a PM localization of Ssy1 (Figure 3A). Instead, we show data supporting that both Ist2 and Ssy1 contain a membrane-tethering module consisting of an ID linker region, a PM-binding domain and a TM domain inserted into the ER. The PMB domain of Ssy1 is composed of a stretch of positive amino acids, which is sufficient to sort soluble GFP and ER-resident TM domains to the PM (Figure 2C,D). The PMB domain of Ssy1 also rescues localization of Ist2 lacking its CSS (Figure 2E). It is not known whether the PMB of Ssy1, like the CSS of Ist2, folds into an amphipathic helix. However, mutagenesis of the PMB introducing residues disrupting amphipatic helix formation did not interfere with the localization of Ssy1(167–283)-TM (data not shown). The interaction partners of the Ssy1 PMB domain are not known yet, but the similarity with the PM-targeting domains present in small GTPases (23) hints toward an electrostatic interaction with PM lipids $PI(4,5)P_2$ and $PI(3,4,5)P_3$.

The native linker regions of Ist2 and Ssy1 are predicted to be ID, and the sorting to the periphery is unaffected when these regions are replaced by a confirmed ID linker domain (Figures 1B and 6B). So, while the native linker region may well have additional functions *in vivo* for which a specific amino acid sequence is required, solely for the targeting, an unrelated ID linker suffices. What is important for localization, however, is the length of the linker regions of Ist2 and Ssy1, because a shorter linker region impairs PM binding (Figures 1B and 6). This may be explained by the fact that a protein with a shorter linker may only find few areas where the PM and the cER are close enough to span the distance between them. But once small membrane associations are formed, additional proteins can probably be congregated at these spots. The strong tethering ability of Ssy1(167–283)-TM is also reflected by the fact that it is able to restore PM–cER contact sites in a strain that lacked any of the proteins mediating the formation of PM–ER junctions (Figure 4) and by the presence of increased amounts of cER underlying the PM in wild-type cells (Figure 5).

The length of the ID regions of Ist2 and Ssy1 differs significantly. With an average distance of approximately 3.5 Å between two consecutive amino acids in a peptide chain, the 340 and 98 residues between the TM domain and the PM-binding region of Ist2 and Ssy1 are able to maximally stretch a distance of 117 and 34 nm, respectively.

With an average distance of 33 nm between the cER and the PM, this region can be sufficient to span the distance between these two compartments. More relevant than these distances of the fully stretched state, are the Stokes radii that we obtained using molecular simulations (Table S1, 24). We calculated that the Stokes radius of the ID region of Ist2 (57.40 ± 4.64 Å) is approximately two times the one of Ssy1 (28.41 ± 2.09 Å). From electron microscopy, we conclude that expression of the PMB domain and ID region of Ssy1 leads to a decreased distance between the cER and the PM, reflecting the shorter Stokes radius. Taken into consideration both the shorter linker and the low expression of native Ssy1, it is more likely that Ssy1 makes use of pre-existing contact sites, while Ist2 may initiate them.

Previous work proposed that Ssy1 binds amino acids extracellularly, inducing a downstream signal (20,25–27). With Ssy1 residing in the ER, we have to reconsider the sensing mechanism of the SPS system. Speculative at this point is that the formation of cytosolic micro-compartments between the ER and the PM may play a role, as was suggested for Ist2 (9). Also, future studies may be directed at identifying putative PM-resident binding partners of the N-terminal region of Ssy1 that is important for the sensor function (15,16,20).

Steric consideration may explain the existence of ID regions in sorting signals of membrane proteins. In contrast to soluble proteins that can move in a three-dimensional manner, membrane proteins are only able to move in two dimensions. Because of its flexibility and length, an ID region gives three-dimensional mobility to a protein terminus encoding a sorting signal, and allows it to extend away from the crowded environment at the membrane and reach over longer distances. If such general considerations indeed apply, then we expect that for more membrane proteins, the sorting relies on an ID linker with terminal sorting motif. Most clearly, this has been shown for Src1/Heh1 and Heh2. Here, a nuclear localization signal together with an ID linker region is required and is sufficient for efficient transport from the ER to the inner nuclear membrane over the nuclear pore complex (15,20,28). In this case, the linker increases spatial freedom of the localization signal to recruit transport factors from the cytoplasm and facilitate transport through the nuclear pore complex. There are also examples where structures other than ID linkers are described to bridge the ER–PM gap, such as the yeast tricalbins Tcb1/2/3, which contains a synaptotagmin-like-mitochondrial-lipid binding protein (SMP) domain (29,30). The mammalian STIM1 protein, of which the extreme C-terminus shows strong similarities with the amphipathic helix of Ist2 in binding PM lipids (29,31), spans the distance between the ER and the PM with cytoplasmic coiled-coil segments of the Orai-activating small fragment (OASF) (32,33).

We speculate that beyond Ist2, Ssy1, Heh1 and Heh2, the sorting of the yeast proteins Scs2, Scs22, Nvj1, Snf3 and YNL046W relies on an ID linker with terminal sorting signal. Scs2 and Scs22 are involved in the formation of contact sites with the PM. Nvj1 is a nuclear envelope-anchored protein that interacts with the vacuolar membrane protein Vac8 to mediate the formation of the nuclear–vacuolar junctions, and Snf3 belongs to the family of glucose transporters and functions as a sensor for low levels of glucose. In mammals, the ER-embedded junctophillins may also have an ID linker region. Here, the N-terminal MORN repeats involved in binding to the PM (34) are separated from the C-terminal TM domain by a so-called divergent region (35), which has low sequence conservation between various isoforms and is predicted to be ID.

Future studies will need to experimentally resolve whether ID domains indeed play a more general role in the functioning and targeting of membrane (anchored) proteins, and in the establishment of heterologous organelle contact sites.

Materials and Methods

Strains and media

All constructs encoding for different Ssy1 variants were transformed into W303 cells. In contrast, those carrying Ist2 chimeras were transformed together with an ER marker protein (encoded by pAK36) into the heterozygous diploid knockout strain *ybr086c*Δ (Thermo Scientific). Stable His^+/Ura^+ transformants were selected and sporulated. Tetrads were dissected on YPD and emerging colonies were replicate plated on selection media containing G418 (200 μg/mL) or lacking histidine or uracil, respectively. The pHK010 construct was transformed into HKY20 (*ssy1*Δ*13*) and HKY29 (*ssy1*Δ*13 shr3*Δ*6*) strains (16, gifts from Dr. Ljungdahl). pAK07 was transformed to the Δtether background (ANDY198, (8), gift from Dr. Emr).

All strains were grown at 30°C in synthetic dropout medium lacking the appropriate amino acids, supplemented with 0.01% adenine for the W303-derived strains and 2% glucose. For induction of the *GAL1* promoter, 2% raffinose and 0.1% galactose were added to the medium instead of glucose.

Plasmid construction

All proteins are expressed from low-copy number plasmids derived from the pUG34 and pUG36 vectors. The plasmids used in this study were generated using standard molecular cloning and PCR techniques. The 3′ end of *IST2* including restriction sites and a randomized ID region were ordered from GeneArt. Detailed description for construction of each plasmid will be provided upon request. A list of the plasmids used in this study can be found in Table S2.

For the cloning of the Ist2 constructs, we have to comment on the She2-dependent transport of *IST2* mRNA to the bud cell. Nucleotides 2716–2777 of *IST2* mRNA form a loop-stem-loop secondary structure containing a CGA triplet in one loop and a highly conserved cytosine in the other loop, and these both are important for the interaction with She2 (36). This transport of *IST2* mRNA to the bud results in an asymmetric localization of Ist2 to the buds of medium- and large-budded cells (37). In order to replace the linker region in Ist2 by a randomized linker, we made a residue substitution at position 919 (T→S). In this way, we replaced the conserved cytosine at position 2757 by a thiamine, abolishing the She2-binding site and also the asymmetric distribution of GFP-Ist2.

Fluorescence microscopy

Imaging of Ssy1-derived proteins was performed on a commercial LSM710 confocal microscope (Zeiss) using a 488 argon ion laser and objective C-Apochromat 40× water immersion objective with 1.2NA. Detection was performed with a PMT. Pixel dwell time for laser-scanning was 0.1 milliseconds with a pixel step of 59 nm. Data were analyzed using the ZEN2010B software package (Carl Zeiss). Imaging of Ist2-derived proteins was performed on a commercial DeltaVision Deconvolution Microscope (Applied Precision), using InsightSSI™ Solid State Illumination of 488 and 594 nm and an Olympus UPLS Apo 100× oil objective with 1.4 NA. Detection was carried out with a CoolSNAP HQ^2 camera. Pixel size was 64 × 64 × 200 nm and data were analyzed with open source software Fiji (38).

Electron microscopy

Cells were precultured in a synthetic drop out medium supplemented with 2% raffinose before inducing expression of the galactose promoter-driven proteins by addition of 0.1% galactose for 16 h. Mid-exponentially growing cells were subsequently fixed, dehydrated, embedded in Spurr's resin and examined by electron microscopy as described in (39).

Membrane fractionation

Membranes of HKY20 and HKY29 expressing HA-tagged Ssy1 (16) were fractionated as described in (40) in the absence of $MgCl_2$ and in the presence of 10 mM EDTA as shown in Figure 3 and Figure S5A,B and in the presence of 1 mM $MgCl_2$ as shown in Figure S5C. EDTA removes Mg^{2+} from the lysate, destabilizing ribosomes, resulting in a lower buoyant density ER membrane that is well resolved from the PM. In short, mid-exponential growing cells were lysed by vortexing with 0.5 mm glass beads (BioSpec products). A slow speed spin removed all the unlysed cells and the soluble fraction containing membranes was separated on a 10–60% sucrose gradient. Equivalents of 18OD units of cells were loaded on top of the gradients.

Acknowledgments

We are grateful to Dr. Ghavami and Dr. Onck for the simulations of the Stokes radii. We thank Dr. Emr for the kind gift of strain ANDY198 and Dr. Ljungdahl for kindly sharing pHK010, HKY20 and HKY29. We thank members of the Veenhoff, Chang and Poolman labs for their valuable discussions. This work is financed by the research programs NWO-Vidi from the Netherlands Organization for Scientific Research (NWO) and by the Netherlands Proteomics Centre.

Supporting Information

Additional Supporting Information may be found in the online version of this article:

Figure S1: Visualization of expression of Ssy1- and Ist2-derived proteins by Western blotting. Ssy1-derived proteins (A) are induced with 0.1% galactose for 4 h. Expression of Ist2-derived proteins (B) was driven by the promoter of Ist2. Cell lysates are prepared from equal amounts of cells and anti-GFP was used for immuno-detection. W303 (A) and ΔIST2 (B) represent the background strains. Bands from full length proteins are indicated by a red dot, GFP-Ssy1 could not be detected by western blot.

Figure S2: The localization pattern of Ist2 at the periphery depends on the length of the intrinsically disordered linker region. The normalized standard deviation of the pixel intensity along the cell periphery of cells expressing different forms of GFP-Ist2. Values are obtained by calculating the standard deviation of the pixel intensities along the periphery of the cell divided by the mean intensity of the cell to correct for expression level differences, in 90 cells per strain. *T*-test between Ist2 and indicated strains: *$p > 0.1$ **$0.1 > p < 0.01$; ***$p < 10^{-5}$.

Figure S3: Colocalization of GFP-Ssy1(167–283)-TM with an mCherry-fused ER-resident protein.

Figure S4: Ultrastructural analysis of W303 expressing Ssy1(191–283)-TM. W303 expressing Ssy1(191–283)-TM appeared to have a strong perinuclear fluorescent signal. Ultrastructural analysis revealed that in these cells, a double layer of ER membrane formed around the nucleus (N) as indicated with an open arrow head. Often at one or two sides of the nucleus, multilamellar ER stacks (closed arrow head) were formed. CW, cell wall; PM, plasma membrane; M, mitochondria. Scale bar represents 200 nm.

Figure S5: Subcellular fractionation of native levels of Ssy1. Membrane fractionation over sucrose gradients of cell lysates of HKY20 (*ssy1Δ13*)

and of cell lysates of HKY29 (*ssy1Δ13 shr3Δ6*) expressing a functional HA-tagged allele of *SSY1* (pHK010). Gradients summarized in (A) and (B) are performed in the same way as described for Figure 3 (in the presence of EDTA) and in both cases, the PM marker Pma1 hardly cofractionates with Ssy1, while the ER marker Dpm1 partly overlaps with Ssy1. Membrane fractionation shown in C is performed in the absence of EDTA and in the presence of 1 mM $MgCl_2$. Ssy1 does not cofractionate with the PM marker Pma1 or the mitochondrial marker (M) Por1. A fraction of the ER marker Dpm1 does cofractionate with Ssy1 (lanes 3 and 4). These fractions were also enriched in nucleoporins (N) recognized by mAb414, but do not overlap with the ribosomal marker (R) Rpl3 that cofractionates with the second ER peak (lanes 10 and 11). The fractions in lanes 3 and 4 may thus present the ribosome-free compartments of the ER, such as those present at the inner nuclear membrane, the pore membrane and the peripheral ER facing the plasma membrane.

Table S1: Stokes radii of indicated intrinsically disordered linker regions from one bead per amino acid molecular dynamic simulations (Ghavami A, et al. Biophys J 2014 Sep 16;107(6):1393 – 1402).

Table S2: Plasmids used in this study.

References

1. Csordas G, Varnai P, Golenar T, Roy S, Purkins G, Schneider TG, Balla T, Hajnoczky G. Imaging interorganelle contacts and local calcium dynamics at the ER-mitochondrial interface. Mol Cell 2010;39:121–132.
2. Geuze HJ, Murk JL, Stroobants AK, Griffith JM, Kleijmeer MJ, Koster AJ, Verkleij AJ, Distel B, Tabak HF. Involvement of the endoplasmic reticulum in peroxisome formation. Mol Biol Cell 2003;14:2900–2907.
3. Pan X, Roberts P, Chen Y, Kvam E, Shulga N, Huang K, Lemmon S, Goldfarb DS. Nucleus-vacuole junctions in *Saccharomyces cerevisiae* are formed through the direct interaction of Vac8p with Nvj1p. Mol Biol Cell 2000;11:2445–2457.
4. Pichler H, Gaigg B, Hrastnik C, Achleitner G, Kohlwein SD, Zellnig G, Perktold A, Daum G. A subfraction of the yeast endoplasmic reticulum associates with the plasma membrane and has a high capacity to synthesize lipids. Eur J Biochem 2001;268:2351–2361.
5. Elbaz Y, Schuldiner M. Staying in touch: the molecular era of organelle contact sites. Trends Biochem Sci 2011;36:616–623.
6. Prinz WA. Bridging the gap: membrane contact sites in signaling, metabolism, and organelle dynamics. J Cell Biol 2014;205:759–769.
7. West M, Zurek N, Hoenger A, Voeltz GKA. 3D analysis of yeast ER structure reveals how ER domains are organized by membrane curvature. J Cell Biol 2011;193:333–346.
8. Manford AG, Stefan CJ, Yuan HL, Macgurn JA, Emr SD. ER-to-plasma membrane tethering proteins regulate cell signaling and ER morphology. Dev Cell 2012;23:1129–1140.
9. Wolf W, Kilic A, Schrul B, Lorenz H, Schwappach B, Seedorf M. Yeast Ist2 recruits the endoplasmic reticulum to the plasma membrane and creates a ribosome-free membrane microcompartment. PLoS One 2012;7:e39703.
10. Lavieu G, Orci L, Shi L, Geiling M, Ravazzola M, Wieland F, Cosson P, Rothman JE. Induction of cortical endoplasmic reticulum by dimerization of a coatomer-binding peptide anchored to endoplasmic reticulum membranes. Proc Natl Acad Sci USA 2010;107:6876–6881.
11. Juschke C, Ferring D, Jansen RP, Seedorf M. A novel transport pathway for a yeast plasma membrane protein encoded by a localized mRNA. Curr Biol 2004;14:406–411.
12. Maass K, Fischer MA, Seiler M, Temmerman K, Nickel W, Seedorf M. A signal comprising a basic cluster and an amphipathic alpha-helix interacts with lipids and is required for the transport of Ist2 to the yeast cortical ER. J Cell Sci 2009;122:625–635.
13. Fischer MA, Temmerman K, Ercan E, Nickel W, Seedorf M. Binding of plasma membrane lipids recruits the yeast integral membrane protein Ist2 to the cortical ER. Traffic 2009;10:1084–1097.
14. Franz A, Maass K, Seedorf M. A complex peptide-sorting signal, but no mRNA signal, is required for the Sec-independent transport of Ist2 from the yeast ER to the plasma membrane. FEBS Lett 2007;581:401–405.
15. Forsberg H, Ljungdahl PO. Genetic and biochemical analysis of the yeast plasma membrane Ssy1p-Ptr3p-Ssy5p sensor of extracellular amino acids. Mol Cell Biol 2001;21:814–826.
16. Klasson H, Fink GR, Ljungdahl PO. Ssy1p and Ptr3p are plasma membrane components of a yeast system that senses extracellular amino acids. Mol Cell Biol 1999;19:5405–5416.
17. Didion T, Regenberg B, Jorgensen MU, Kielland-Brandt MC, Andersen HA. The permease homologue Ssy1p controls the expression of amino acid and peptide transporter genes in *Saccharomyces cerevisiae*. Mol Microbiol 1998;27:643–650.
18. Iraqui I, Vissers S, Bernard F, de Craene JO, Boles E, Urrestarazu A, Andre B. Amino acid signaling in *Saccharomyces cerevisiae*: a permease-like sensor of external amino acids and F-Box protein Grr1p are required for transcriptional induction of the AGP1 gene, which encodes a broad-specificity amino acid permease. Mol Cell Biol 1999;19:989–1001.
19. Nelissen B, De WR, Goffeau A. Classification of all putative permeases and other membrane plurispanners of the major facilitator superfamily encoded by the complete genome of *Saccharomyces cerevisiae*. FEMS Microbiol Rev 1997;21:113–134.
20. Bernard F, Andre B. Genetic analysis of the signalling pathway activated by external amino acids in *Saccharomyces cerevisiae*. Mol Microbiol 2001;41:489–502.
21. Kota J, Gilstring CF, Ljungdahl PO. Membrane chaperone Shr3 assists in folding amino acid permeases preventing precocious ERAD. J Cell Biol 2007;176:617–628.
22. Kuehn MJ, Schekman R, Ljungdahl PO. Amino acid permeases require COPII components and the ER resident membrane protein Shr3p for packaging into transport vesicles in vitro. J Cell Biol 1996;135:585–595.
23. Heo WD, Inoue T, Park WS, Kim ML, Park BO, Wandless TJ, Meyer T. PI(3,4,5)P3 and PI(4,5)P2 lipids target proteins with polybasic clusters to the plasma membrane. Science 2006;314:1458–1461.
24. Ghavami A, van der Giessen E, Onck PR. Coarse-grained potentials for local interactions in unfolded proteins. J Chem Theory Comput 2012;9:432–440.

25. Gaber RF, Ottow K, Andersen HA, Kielland-Brandt MC. Constitutive and hyperresponsive signaling by mutant forms of *Saccharomyces cerevisiae* amino acid sensor Ssy1. Eukaryot Cell 2003;2:922–929.
26. Poulsen P, Gaber RF, Kielland-Brandt MC. Hyper- and hyporesponsive mutant forms of the *Saccharomyces cerevisiae* Ssy1 amino acid sensor. Mol Membr Biol 2008;25:164–176.
27. Wu B, Ottow K, Poulsen P, Gaber RF, Albers E, Kielland-Brandt MC. Competitive intra- and extracellular nutrient sensing by the transporter homologue Ssy1p. J Cell Biol 2006;173:327–331.
28. Meinema AC, Laba JK, Hapsari RA, Otten R, Mulder FA, Kralt A, van den BG, Lusk CP, Poolman B, Veenhoff LM. Long unfolded linkers facilitate membrane protein import through the nuclear pore complex. Science 2011;333:90–93.
29. Park CY, Hoover PJ, Mullins FM, Bachhawat P, Covington ED, Raunser S, Walz T, Garcia KC, Dolmetsch RE, Lewis RS. STIM1 clusters and activates CRAC channels via direct binding of a cytosolic domain to Orai1. Cell 2009;136:876–890.
30. Toulmay A, Prinz WA. A conserved membrane-binding domain targets proteins to organelle contact sites. J Cell Sci 2012;125:49–58.
31. Ercan E, Momburg F, Engel U, Temmerman K, Nickel W, Seedorf M. A conserved, lipid-mediated sorting mechanism of yeast Ist2 and mammalian STIM proteins to the peripheral ER. Traffic 2009;10:1802–1818.
32. Yang X, Jin H, Cai X, Li S, Shen Y. Structural and mechanistic insights into the activation of Stromal interaction molecule 1 (STIM1). Proc Natl Acad Sci USA 2012;109:5657–5662.
33. Yu F, Sun L, Courjaret R, Machaca K. Role of the STIM1 C-terminal domain in STIM1 clustering. J Biol Chem 2011;286:8375–8384.
34. Takeshima H, Komazaki S, Nishi M, Iino M, Kangawa K. Junctophilins: a novel family of junctional membrane complex proteins. Mol Cell 2000;6:11–22.
35. Garbino A, van Oort RJ, Dixit SS, Landstrom AP, Ackerman MJ, Wehrens XH. Molecular evolution of the junctophilin gene family. Physiol Genomics 2009;37:175–186.
36. Olivier C, Poirier G, Gendron P, Boisgontier A, Major F, Chartrand P. Identification of a conserved RNA motif essential for She2p recognition and mRNA localization to the yeast bud. Mol Cell Biol 2005;25:4752–4766.
37. Takizawa PA, DeRisi JL, Wilhelm JE, Vale RD. Plasma membrane compartmentalization in yeast by messenger RNA transport and a septin diffusion barrier. Science 2000;290:341–344.
38. Schindelin J, Arganda-Carreras I, Frise E, Kaynig V, Longair M, Pietzsch T, Preibisch S, Rueden C, Saalfeld S, Schmid B, Tinevez JY, White DJ, Hartenstein V, Eliceiri K, Tomancak P, et al. Fiji: an open-source platform for biological-image analysis. Nat Methods 2012;9:676–682.
39. Griffith J, Mari M, De MA, Reggiori F. A cryosectioning procedure for the ultrastructural analysis and the immunogold labelling of yeast *Saccharomyces cerevisiae*. Traffic 2008;9:1060–1072.
40. Roberg KJ, Rowley N, Kaiser CA. Physiological regulation of membrane protein sorting late in the secretory pathway of *Saccharomyces cerevisiae*. J Cell Biol 1997;137:1469–1482.